Functional Materials Letters
(2022) 2250026 (5 pages)

DOI: 10.1142/S1793604722500266

World Scientific
www.worldscientific.com

Flexible capacitive three-dimensional force sensor for hand motion capture and handwriting recognition

Zihan Lv,[*] Zeqian Song,[*] Diqing Ruan,[*] Huaping Wu[†] and Aiping Liu[*,‡]

[*]*Key Laboratory of Optical Field Manipulation of Zhejiang Province*
Zhejiang Sci-Tech University, Hangzhou 310018, P. R. China

[†]*Key Laboratory of Special Purpose Equipment and Advanced Processing Technology*
Ministry of Education and Zhejiang Province, College of Mechanical Engineering
Zhejiang University of Technology, Hangzhou 310023, P. R. China

[‡]*liuaiping1979@gmail.com*

Received 12 August 2022; Accepted 16 September 2022; Published 10 October 2022

Handwriting recognition has been widely studied as an important signal transmission method in the field of human–computer interaction. Flexible capacitive three-dimensional (3D) force sensor is widely used in this field because of its high sensitivity, large dynamic response range and good mechanical stability. However, traditional flexible capacitive 3D force sensors based on the array structure usually only sense 3D force with equivalent forward pressure rather than the decoupling of real 3D force in space. Herein, we design a flexible capacitive 3D force sensor with petal-like electrode to capture various hand movements in 3D space and further decouple 3D force to 1D force along *X*, *Y* and *Z* directions. The sensor presents a high sensitivity (1.1 kPa^{-1} at the pressures below 1 kPa), a fast response (63 ms) and excellent repeatability under continuous pressure. In addition, the electrode with eight-petal structure helps simplify the decoupling process of 3D force. Through handwriting test, the sensor presents good sensing performance for hand motion capture and handwriting recognition, which is expected to be applied in the field of human–computer interaction.

Keywords: Three-dimensional force; capacitive sensing; flexible sensor; handwriting recognition.

With the continuous development of human–computer interaction technology, handwriting recognition has been widely studied as a way for people to interact with machines through hand movements.[1–3] Due to the complexity of human hand movement, it is difficult to capture hand movement signals in time, and an applicable flexible sensor[4] as the medium of this interaction mode is necessary. Flexible capacitive three-dimensional (3D) force sensor with conformal with the skin of the hand, high sensitivity,[5–7] large dynamic response range[8–11] and good mechanical stability[12,13] has the function of simultaneously detecting 3D force information[14–17] when compared with ordinary 1D force sensor, therefore is widely used in the field of handwriting recognition. There are many kinds of flexible capacitive 3D force sensors. For example, a flexible 3D force sensor based on ZnO nanowires array structure was designed by Chen.[18] By changing the upper and lower plates spacing, an equivalent 3D force with forward force but not a real 3D spatial force was detected. Rocha proposed a capacitive three-axis force sensor with a sandwich structure,[19] and the information of 3D force was really reflected by a complex derivation process after calibrating the 3D forces. Though the methods based on equivalent 3D force along forward force or complex decoupling of the real 3D forces can provide the spatial information of 3D forces, a flexible capacitive 3D force sensor with ingenious design is still imperative and challenging for real 3D force recognition and hand motion capture via simplified decoupling way.

Herein, we propose a flexible capacitive 3D force sensor with array electrodes of petal-like structure. Attributing to the unique structure of the sensor, the forward force and tangential force can be separated detected, so as to further decouple the 3D force applied on the sensor. We analyze the basic sensing performance of the sensor, demonstrating its good sensing sensitivity and excellent recognition capability by a practical handwritten test. This work provides an ingenious strategy for the fabrication of flexible capacitive 3D force sensor with broad application prospects in human–computer interaction and wearable devices.

Figure 1 shows the synthesis scheme for flexible capacitive 3D force sensor, which contained two copper electrode layers (eight petal-shaped top electrodes and round bottom electrode) and a media layer (composed of 4 wt.% Ecoflex and multi-walled carbon nanotubes with 95% purity). For a typical preparation process, the pre-prepared Ecoflex

‡Corresponding author.

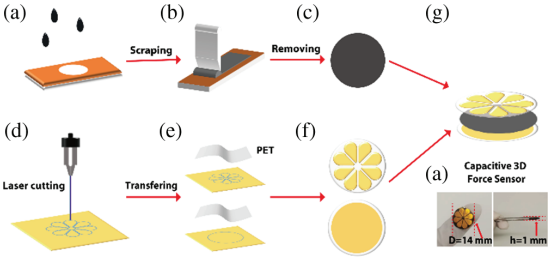

Fig. 1. Preparation process of flexible capacitive 3D force sensor. (a) Pour the mixed solution to the mold and (b) scrape and dry. (c) The media layer after demolding. (d) Laser cutting copper tape and (e) transferring it onto PET to obtain electrode layers (f). (g) Assembled sensor with a diameter of 14 mm and a thickness of 1 mm (h).

solution and carbon nanotubes solution dispersed in xylene were mixed and stirred thoroughly, and then the mixed solution was poured into the well-prepared medium layer mold to scratch and smear using a scraper and kept at 80°C for 1 h before demolding (Figs. 1(a)–1(c), Fig. S1(a)). The adhesive copper tape on one side with a thickness of 150 μm was cut by a laser cutting machine and transferred to flexible PET substrate to form the well-designed electrode layer (Figs. 1(d)–1(f), Figs. S1(b) and S1(c)). The electrode layers and media layer were further assembled by the uncured Ecoflex and then cured at 80°C for 1 h, and the copper wires were adhered to the extension of electrode layers via the conductive silver paste for electrical signal output (Fig. S1(d)). The flexible capacitive 3D force sensor has a diameter of 14 mm and a thickness of 1 mm (Figs. 1(g) and 1(h)), which fits well with the finger size for handwriting (Fig. S1(d)).

The capacitance at corresponding time for the sensor was collected by a digital bridge (LCR) at the frequency of 100 kHz and a constant voltage of 1V via the conductive silver paste to contact the extension of electrode layers (Figs. S1(d) and S2). During the test, the sensor was placed on the displacement platform with *X*-, *Y*- and *Z*-axes, and then positive and tangential forces were applied to the sensor by the mechanical test platform to detect the sensing performance of the sensor and calibrate the 3D forces. The mechanical test platform consists a mechanical testing machine for normal force infliction and a linear moving platform for tangential force infliction (Fig. S3). The linear moving platform concluded a slide table and a dynamometer. The mechanical testing machine was controlled by the computer programming, and the microcontroller drived the motor to control the movement of the slide. The acrylonitrile–butadiene–styrene (ABS) slopes with different angles were prepared by 3D printing technology and used to place sensor in the 3D force test experiment.

Figures 2(a) and 2(b) show the relative capacitance change ($\Delta C/C_0 = (C - C_0)/C_0$) of the flexible capacitive 3D force sensor when the tangential force and the forward force are applied to one unit of the petal-shaped top electrode on the sensor,

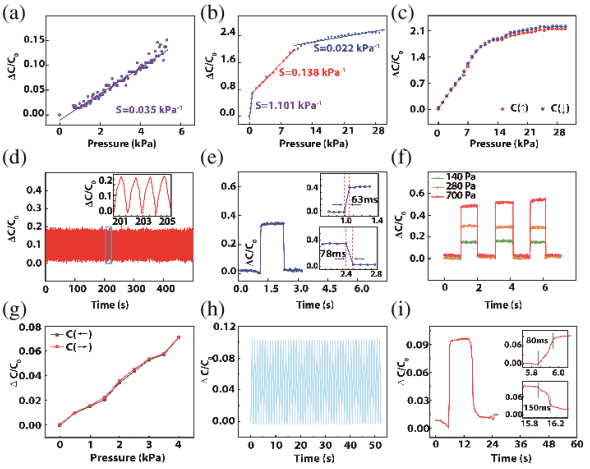

Fig. 2. Detection of the basic sensing performance of the sensor when the tangential and forward force are applied to one unit of the petal-shaped top electrode on the sensor. (a) Tangential sensitivity of sensor. (b) Forward sensitivity of the sensor. (c) Hysteresis of the sensor at a positive pressure ranging from 0 to 30 kPa. (d) Stability of the sensor during 500 cycle tests under 200 Pa positive pressure. (e) Response time of the sensor under 300 Pa positive pressure. (f) Repeatable responses of the sensors under different positive pressures. (g) Hysteresis of the sensor at a tangential pressure ranging from 0 to 4 kPa. (h) Tangential stability of the sensor during 50 cycle tests under 4 kPa tangential pressure. (i) Response time of the sensor under 4 kPa tangential pressure.

respectively. The sensitivity of capacitive sensor (S) is defined by $S = \delta(\Delta C/C_0)/\Delta P$, where P is the applied pressure, C and C_0 are the capacitances with and without pressure, respectively. By fitting the capacitance as a function of time, the tangential sensitivity of 0.035 kPa^{-1} and the maximal forward sensitivity of 1.101 kPa^{-1} for the sensor are obtained. This sensitivity is sufficient for hand motion capture and handwriting recognition. In addition, the robustness and stability are also very important in practical applications. The hysteresis of the flexible capacitive 3D force sensor was measured when the sensor was loaded and unloaded at a positive pressure ranging from 0 to 30 kPa, presenting good hysteresis and robustness (Fig. 2(c)). The sensor maintains stable sensing signal without fatigue during 500 repeated loading–unloading cycles (programmed through the mechanical test platform) under 200 Pa positive pressure, indicating its excellent stability (Fig. 2(d)). The sensor displays a rapid response upon positive pressure of 300 Pa with the loading time of 63 ms and the unloading time of 78 ms (Fig. 2(e)) and good repeatability at different positive pressures (140 Pa, 280 Pa and 700 Pa in Fig. 2(f)). The excellent tangential hysteresis of sensor is also verified at a tangential pressure ranging from 0 to 4 kPa (Fig. 2(g)), presenting satisfactory tangential stability of the sensor during 50 tangential force (4 kPa) cycles (Fig. 2(h)) and fast response ability to 4 kPa tangential force (loading time of 80 ms and unloading time of 150 ms in Fig. 2(i)). The linear detection ranges of the sensor are 0–50 N for the forward force and 0–4 N for the tangential force (Fig. S4).

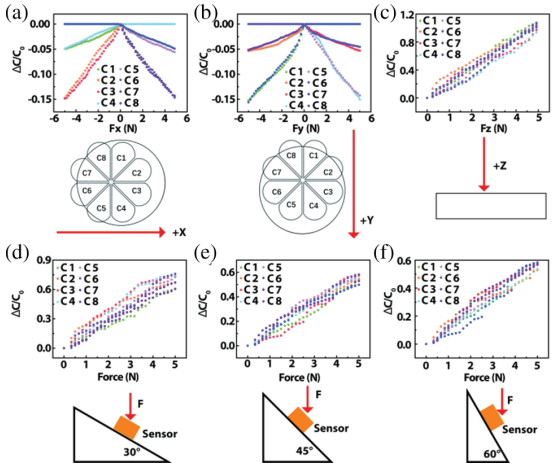

Fig. 3. Calibration and testing of 3D forces. Calibration in the (a) *X*, (b) *Y* and (c) *Z* directions. 3D force with (d) 30°, (e) 45° and (f) 60° included angle to the sensor surface is applied to the sensor.

When a 3D force at some angle to the *X*-axis, *Y*-axis or *Z*-axis is applied to the whole flexible capacitive 3D force sensor, the sensing signal needs to be calibrated. When a 0–5 N force is applied to the *X*, *Y* and *Z* directions of the sensor, respectively, the change of the output capacitance of the sensor is detected and shown in Figs. 3(a)–3(c). No matter the top electrode of the sensor moves in any direction, only part of the bottom electrode will change the projected area with the top electrode, which is the unique feature of this structure. We can determine the application range of 3D forces by observing the change of projection area of top electrode plate relative to the common bottom electrode plate, separate the forward and tangential forces at the same time, and decouple the 3D forces by the decoupling matrix. The output capacitive value of the top and bottom electrodes with displacement is given by

$$C_t = \varepsilon_r \varepsilon_0 \frac{s}{d + \Delta d}, \tag{1}$$

$$C_b = \varepsilon_r \varepsilon_0 \frac{s + \Delta s}{d + \Delta d}. \tag{2}$$

Here Δd is the change in distance between the top and bottom electrodes, Δs is the change of projection area of top and bottom electrodes, ε_0 is the dielectric constant of air ($\varepsilon_0 = 1 \times 10^{-12}$ F/m), and ε_r is the dielectric constant of media ($\varepsilon_r = 9.8 \times 10^{-12}$ F/m). Then, the 3D force can be decoupled into a forward force and a tangential force only by the derivation of the formula. According to the calibration results, a decoupling matrix of positive forces (3D force calibration along the *Z* axis) can be obtained

$$[\mathrm{Fz}] = \begin{bmatrix} 1.191 & 1.191 & 1.191 & 1.191 \end{bmatrix} * [A]. \tag{3}$$

The transposed matrix of relative capacitance change can be written as follows:

$$[A]^T = \begin{bmatrix} \frac{\Delta C\mathrm{a}}{C\mathrm{a}} & \frac{\Delta C\mathrm{b}}{C\mathrm{b}} & \frac{\Delta C\mathrm{c}}{C\mathrm{c}} & \frac{\Delta C\mathrm{d}}{C\mathrm{d}} \end{bmatrix}, \tag{4}$$

where the ΔCa, ΔCb, ΔCc, ΔCd (a–d are the unit numbers in top electrode) indicate the relative change in the capacitance of the top and bottom electrodes that do not produce the change of the projected area, respectively. Using Eq. (2) minus Eq. (1), we can get the output capacitance when the two electrodes produce planar movement

$$C = \varepsilon_r \varepsilon_0 \frac{\Delta s}{d + \Delta d}. \tag{5}$$

According to the calibration results, the decoupling matrix of tangential force (3D force calibration along the *X*- and *Y*-axes) is given as follows:

$$\begin{bmatrix} Fx+ \\ Fx- \end{bmatrix} = \begin{bmatrix} 3.246 & 1.084 & 1.084 & 3.246 \\ -3.141 & -1.127 & -1.127 & -3.141 \end{bmatrix} * [B], \tag{6}$$

$$\begin{bmatrix} Fy+ \\ Fy- \end{bmatrix} = \begin{bmatrix} 1.118 & 3.285 & 3.285 & 1.118 \\ -3.166 & -1.072 & -1.072 & -3.166 \end{bmatrix} * [B], \tag{7}$$

$$[B]^T = \begin{bmatrix} \frac{\Delta C\mathrm{d}}{C\mathrm{d}} & \frac{\Delta C\mathrm{e}}{C\mathrm{e}} & \frac{\Delta C\mathrm{f}}{C\mathrm{f}} & \frac{\Delta C\mathrm{g}}{C\mathrm{g}} \end{bmatrix}. \tag{8}$$

Here ΔCd, ΔCe, ΔCf, ΔCg (d–g are the unit numbers in top electrode) indicate the relative change in the capacitance of the top and bottom electrodes that produce the change of the projected area, respectively. The $[B]$ is the matrix of relative capacitance change.

In order to verify the accuracy of the decoupling equation, a linearly varying force of 0–5 N at 30°, 45° and 60° is applied to the sensor, respectively (Figs. 3(d)–3(f)). Comparing the calculated value of the 3D force decoupling and the actual applied force, all errors are controlled within 6% (Table S1). This demonstrates the accuracy of decoupling method of the 3D force sensor for potential application in practical situations.

Besides, we also studied the effect of unit number of top electrode (4, 8 and 12) on the sensor performance. The results shown in Fig. S5 indicate that as the unit number of top electrode increases, the error of decoupling is decreasing. However, the number of decoupling matrix columns is also increasing, leading to increased decoupling difficulty. Therefore, in the case of ensuring the accuracy of the decoupling, the sensor with eight units on the top electrode is optimized for the improvement of sensing performance and decoupling efficiency of the 3D force sensor.

The sensor's performance in actual handwriting recognition is further probed into. The sensor is first fixed to the finger pulp of index finger and a given force (about 5 N) is applied to the sensor through the finger. Then, the user's writing information is judged by capturing the waveform

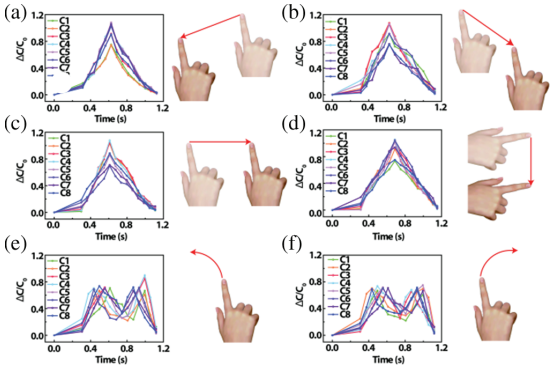

Fig. 4. Relative capacitive change of flexible capacitive 3D force sensor when the sensor is fixed to the finger pulp of index finger to write six commonly used strokes. Write along the diagonal lines of 45° (a) and 135° (b). Write along the lines of 0° (c) and 90° (d). Write along the counterclockwise (e) and clockwise curves (f).

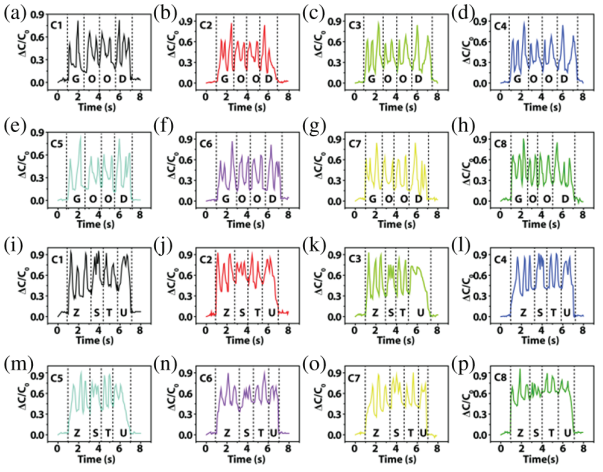

Fig. 5. Handwriting recognition using flexible capacitive 3D force sensor. (a)–(h) Relative capacitive change of C1–C8 units when writing "GOOD". (i) – (p) Relative capacitive change of C1–C8 units when writing "ZSTU".

and peak value of the relative capacitance change curve of the sensor. As shown in Fig. 4, six commonly used strokes are tested when the finger writes along the diagonal lines of 45° and 135°, horizontal 0° and vertical 90°, clockwise and counterclockwise curves, respectively, and the obtained peak shape and intensity are not exactly the same for the 3D force sensor with eight units of petal-shaped array. When the stroke is a straight line with 45°, such as Fig. 4(a), the peak value of relative capacitive change produced by C1 and C2 units are maximal because the relative displacement of top and bottom electrodes is maximal in the location of C1 and C2. There is also a relative displacement at C3 and C8 units with the bottom electrode, but the amplitude is relative little compared to those of C1 and C2, presenting a less capacitance change. Since there is no relative displacement at C4, C5, C6, C7 with the bottom electrode, they only have capacitance change induced by distance change between two electrode plates, so the peak value of the capacitance change is minimal. For the curve stroke, such as Fig. 4(e), the relative displacement of the top and bottom electrode plates will go through a tendency to increase, decrease, and then increase, thus the waveform of the relative capacitance change also takes on the shape of "M". Due to the symmetry of the curved motion, the waveform and peak of the output curve of each electrode plate are approximately the same. These results hint that different letters or words with various strokes could be distinguished by combining the characteristics of waveforms and peaks corresponding to different strokes.

Figure 5 shows the relative capacitance change curves of C1–C8 units when the testers writing the English words "GOOD" and "ZSTU" (the acronym of Zhejiang Sci-Tech University in China), respectively. The capacitance change curves of each letters can be of good consistence with the combination of corresponding strokes. This proves that the flexible capacitive 3D force sensor designed in this work has good application potential in the field of wearable handwriting recognition.

In order to verify the accuracy of handwriting recognition, we calculated the waveform similarity of the relative capacitance change for letters "A" to "G", plotting the similarity matrix based on the calculation result (Fig. S6). The lighter the color, the smaller the value, the greater the similarity, hinting the accuracy of handwriting recognition by the 3D force sensor. Furthermore, in practical applications, the applied force and tilt angle of each person's finger when writing are different. To verify whether these factors have an impact on sensor performance, we applied a force to the sensor to make the sensor move along the diagonal lines of 45°. We tested the sensing signals by applying a force (0.5 N, 1 N, 1.5 N and 2 N) to the sensor in a 45° tilt angle or applying a 2 N force to the sensor at different tilt angles (15°, 30°, 45° and 60°). The relative capacitance changes are shown in Fig. S7. By using the 3D force decoupling formula, the actual movement directions of the sensor are calculated (Tables S2 and S3) with the errors within 5° when compared to the predetermined direction of motion (diagonal lines of 45°). We also calculate the errors between the actual and calculated tilt angles at different forces and the errors between the actual and calculated forces at different tilt angles (within 2.5° in Table S2 and 0.1 N in Table S3). This indicates that the capture of the sensor's trajectory is accurate. Therefore, the applied force and the tilt angle of fingers when writing do not have obvious impact on the sensing performance of the 3D force sensor.

In summary, we have proposed a flexible capacitive 3D force sensor consisting of a common electrode as the bottom plate and a petal-shaped array electrode as the top plate.

The sensor with high sensitivity (1.101 kPa^{-1} at pressures below 1 kPa) and fast response time (63 ms) under steady pressure can directly decouple complex 3D forces into forward and tangential forces with reduced difficulty of decoupling via the designed unique structure, giving an error of less than 6% when compared to the experimental values. The designed sensor also shows good sensing performance and excellent practicality in actual handwriting recognition experiments, indicating its application potential in the field of human–computer interaction and wearable devices.

Acknowledgments

This work was supported by the Zhejiang Outstanding Youth Fund of China (No. LR19E020004), the Youth Top-notch Talent Project of Zhejiang Ten Thousand Plan of China (No. ZJWR0308010) and the Zhejiang Provincial Natural Science Foundation of China (No. LR20A020002).

References

1. S. Rautaray *et al*., *Artif. Intell. Rev*. **43**, 1 (2015).
2. S. Impedovo *et al*., *Pattern Recognit.* **47**, 916 (2014).
3. A. Moin *et al*., *Nat. Electron.* **4**, 54 (2021).
4. S. W. Lu *et al*., *Funct. Mater. Lett.* **13**, 2051002 (2020).
5. I. You *et al*., *Science* **370**, 961 (2020).
6. Y. C. Huang *et al.*, *Nat. Electron*. **3**, 59 (2020).
7. X. Tao *et al*., *Nano Lett*. **15**, 7281 (2015).
8. J. Wang *et al.*, *ACS Appl. Mater. Interfaces* **11**, 11928 (2019).
9. H. Qin *et al*., *J. Mater. Chem. C* **7**, 601 (2019).
10. B. Nie *et al*., *Mater. Horiz.* **8**, 962 (2021).
11. Y. Zhang *et al.*, *ACS Appl. Mater. Interfaces* **12**, 27961 (2020).
12. C. Pang *et al*., *Nat. Mater*. **11**, 795 (2012).
13. L. Ma *et al*., *J. Mater. Chem. C* **6**, 13232 (2018).
14. S. C. B. Mannsfeld *et al*., *Nat. Mater*. **9**, 859 (2010).
15. R. Shi *et al*., *Sci. China Mater*. **61**, 1587 (2018).
16. J. Yang *et al*., *ACS Appl. Mater. Interfaces* **11**, 14997 (2019).
17. S. Y. Kim *et al*., *Adv. Mater*. **27**, 4178 (2015).
18. Y. S. Chen *et al*., *Science* **353**, 678 (2016).
19. J. G. Rocha *et al*., *IEEE Trans Instrum. Meas*. **58**, 2830 (2009).